International Journal of Numerical Methods and Applications

https://pphmjopenaccess.com
https://doi.org/10.17654/0975045226001
Volume 26, Number 1, June 2026, Pages 1-38 **P-ISSN: 0975-0452**

NUMERICAL ANALYSIS OF A FOUR-STAGE AGE-STRUCTURED POPULATION DYNAMICS MODEL WITH SPATIAL DIFFUSION FOR DESERT LOCUSTS

Nestor RAMDE[1,2,*], Amidou TRAORE[3,4], Seydou SORE[5], Yacouba SIMPORE[1,6] and Ousseynou NAKOULIMA[2]

[1]Laboratoire Analyse Numérique, Informatique et Biomathématiques (LANIBIO)
UFR, Sciences Exactes et Appliquées
Université Joseph KI-ZERBO
03 BP 7021 Ouagadougou 03, Burkina Faso
e-mail: ramdegnestor@gmail.com

[2]Laboratoire MAINEGE
UFR, Sciences et Technique
Université Ouaga 3S
03 BP 7021 Ouagadougou 03
Burkina Faso
e-mail: onakouli@gmail.com

Received: June 2, 2025; Revised: July 18, 2025; Accepted: July 30, 2025
2020 Mathematics Subject Classification: 65N06, 65N12, 65N22, 65M06, 65J08, 65J1.
Keywords and phrases: numerical solutions, desert locusts, convergence, finite differences.
*Corresponding author

How to cite this article: Nestor RAMDE, Amidou TRAORE, Seydou SORE, Yacouba SIMPORE and Ousseynou NAKOULIMA, Numerical analysis of a four-stage age-structured population dynamics model with spatial diffusion for desert locusts, International Journal of Numerical Methods and Applications 26(1) (2026), 1-38.
https://doi.org/10.17654/0975045226001

Published Online: September 1, 2025

[3]Laboratoire Sciences et Technologies (LaST)
UFR, Sciences et Techniques
Université Thomas SANKARA
12 BP 417 Ouagadougou 12
Burkina Faso
e-mail: samidoutraore@gmail.com

[4]Laboratoire Interdisciplinaire de Recherche en
Sciences Appliquées (LIRSA)
École Normale Supérieure (ENS)
Burkina Faso

[5]Laboratoire de Mathématiques, Informatique et Application (LAMIA)
Université Norbert ZONGO de Koudougou
Burkina Faso
e-mail: seydousore27@gmail.com

[6]Université Yembila Abdoulaye TOGUYENI
Burkina Faso
e-mail: simpore.yacouba@gmail.com

Abstract

Consider a linear system of a locust population dynamics model structured on age, space with non-local boundary conditions. The behavior of the terms of the numerical solutions of this model is studied using the finite difference method, as well as the convergence (consistency and stability) of the method. Numerical illustrations of the schemes are proposed.

1. Introduction

Pest insects represent a major threat to agricultural production in many regions of the world, particularly in the Sahel, where food self-sufficiency and crop protection remain unresolved challenge. During invasion periods,

no crop is spared, and losses can reach several tens of thousands of tons per day. Among these pests, the desert locust, Schistocerca gregaria (Orthoptera: Acrididae), stands out as a notorious migratory insect known for its ability to form vast mobile swarms able to travel long distances. These swarms cause severe agricultural damage, exacerbate food insecurity, and lead to significant economic losses. The species is found in the desert and arid regions of Africa, the Arabian Peninsula, and parts of Southwest Asia, see Cressman [5], Kimathi et al. [10] and Showler [19]. Each individual measures between 7 and 8 cm in length and weighs approximately 2 g. It undergoes five molts during the gregarious phase and six during the solitary phase. The locust life cycle generally is subdivided into three stages: eggs, nymphs (or larvae) and adults, see the work of Guan et al. [8] and Symmons and Cressman in [23]. In this article, we examine the impact of growth variations within a locust population. To do this, we propose a numerical simulation of the population dynamics, modeled using partial differential equations structured around the different development stages. Population dynamics, often studied by biologists, has long interested mathematicians because of the theoretical challenge it poses and the possibilities it offers for numerical simulations. The evolution of a population in a given region depends on various factors, including egg-laying, birth rates, mortality and migration. It has been shown that these biological parameters are essential for modelling and satisfy the existence and uniqueness properties in a previous study, see [17]. Mathematics commonly uses the notions of infinite and continuous. Approximate solutions are ultimately calculated as collections of discrete values in the form of components of a solution vector of a matrix problem. In order to move from an exact (continuous) problem to an approximate (discrete) problem, several techniques are available: finite differences, finite elements and finite volumes. In this article, we will use the finite difference method for our solution. The finite difference method consists in replacing the derivatives appearing in the continuous problem by divided differences or combinations of point values of the function at a finite

number of discrete points or mesh nodes. The aim of this manuscript is to present numerical simulations of (1.1)-(1.2) which is the locust population dynamics model, while ensuring that the solution remains non-negative. In addition, we study the convergence of the chosen method. For this, we can, for example, refer to the work of Traore et al. in [25] where they established the existence and uniqueness of the solution of their problem and carried out numerical simulations of their model using the finite difference method, but unlike our model, their model has no space variable, and they also did not study the convergence of their method. Also see in [20], the work of Simporé where he worked on the null controllability of an age-structured model with spatial diffusion, including numerical applications but unlike our method, he did not study the convergence of his method. Similarly, Gilioli et al. [7] studied the numerical aspect of their model without studying the convergence of the method. Other significant contributions include those by Mechhoud et al. [13]; Pasquali et al. [15], which enhanced numerical approaches and graphical representations of population models. Fundamental studies, such as those by Lax and Richtmyer [12], investigated the numerical resolution of initial value problems and convergence using finite difference methods. O'Brien et al. [14] highlighted stability in connection to rounding errors. More recently, Ren et al. [18] demonstrated the optimal convergence of their scheme in the L^2 norm, and Lagrée [27] addressed numerical and convergence issues in these problems. We can also highlight the work of Courant et al. in [4], demonstrated that a sufficiently flexible finite difference scheme can provide a numerical solution while also addressing the convergence of the numerical procedure. This research is fundamental in numerical analysis, particularly for partial differential equations, as it offers valuable insights into balancing flexibility, accuracy, and stability in numerical solutions. We also note that in [26], Traoré and his collaborators enhanced their model with numerical simulations. These contributions are particularly significant as they demonstrate the relevance of their approach while validating the theoretical results through detailed and illustrative visual

representations. In [9], Kim and Park studied the asymptotic behavior of numerical solutions for a model describing the dynamics of an age-structured population. They also conducted numerical experience to illustrate their results and validate their analyses. In reference [11], Lanzarone et al. proposed a Bayesian approach to estimate the probability density functions of parameters associated with the extrinsic mortality rate, using population abundance data. Their study also incorporates simulated data to assess the convergence of the proposed algorithm. The work of Traoré et al. [24] focusing on the study of null controllability properties of an age-structured population dynamics model with nonlocal boundary conditions, concluded with numerical illustrations validating the theoretical findings. We can also refer to reference [21], where Simporé, in his study on the null controllability of a nonlinear population dynamics model, highlights numerical simulations provided as illustrative examples. It should be noted that in [1], Angulo et al. through their new numerical method for approximating the solutions of a non-autonomous form of the classical Gurtin-MacCamy population dynamics model, with a mortality rate consisting of an intrinsic age-dependent rate that becomes unbounded when age approaches its maximum value, combined with a non-local, non-autonomous, bounded rate dependent on the weighted population size. They also present the results of several numerical simulations. In [16], Picart and Ainseba presented a numerical analysis approach to solve a parameter identification problem. We also cite Fernandez-Cara et al. in [6], whose main objective is to numerically compute a control that leads to a numerical approximation of the state from initial data prescribed exactly at zero, and who have also proposed numerical schemes. We also refer to Simpore and Tambue [22], who proposed a new numerical technique combining spatial discretization by finite differences-finite elements and temporal discretization by exponential integrator, illustrated by numerical simulations. They established the convergence of their numerical method and concluded their study with several numerical applications, effectively demonstrating the robustness and efficiency of their approach. It

is also worth noting that in the works of Courant et al. ([2] and [3]), it is established that the CFL (Courant-Friedrichs-Lewy) condition is a necessary requirement to ensure the convergence of a numerical scheme. This condition, which we have meticulously adhered to in our study, plays a fundamental role in the analysis of stability and consistency of numerical methods.

The specificity of our numerical simulations, compared with other similar models, lies in the very structure of our approach. Unlike conventional models, which generally consider the first derivative in terms of age and time, or in terms of age, time and diffusion in terms of age, or even in terms of age, time and diffusion in terms of space for numerical simulations, our model simultaneously incorporates diffusion terms in both age and space, which makes numerical simulations of our model interesting. This particularity allows us to better capture complex phenomena and significantly enriches the dynamics represented. In this context, we propose various schemes and numerical simulations for our model. The main objective of this manuscript is to use the finite difference method to discretize the age (b) and space (x) variables, which will make it easier to obtain the matrix for the illustrative figures. At the same time, we establish the convergence of the method used, showing its consistency and stability. Our study is structured into three main sections. In the second section, we present the model along with the main results, including the discretization schemes and matrices used for graphical representations. Finally, in the last section, we provide detailed numerical illustrations to support our conclusions. This study builds upon the previous work of Ramdé et al. [17], has a particular emphasis on numerical aspects.

Consider the locust population dynamics model presented in [17]:

$$
\begin{cases}
\partial_t y_1(b,t,x)+\partial_b[v_1(b,T(t),x)\,y_1(b,t,x)] \\
-\beta\partial_b^2 y_1(b,t,x)-\mu_1\Delta y_1(b,t,x) \\
=-[\theta_1(b,T(t),x)+\gamma_1(b,T(t),x)]\,y_1(b,t,x), & (b,t,x)\in\alpha_1, \\
\partial_t y_2(b,t,x)+\partial_b[v_2(b,T(t),x)\,y_2(b,t,x)] \\
-\beta\partial_b^2 y_2(b,t,x)-\mu_2\Delta y_2(b,t,x) \\
=-[\theta_2(b,T(t),x)+\gamma_2(b,T(t),x)]\,y_2(b,t,x), & (b,t,x)\in\alpha_2, \\
\partial_t y_3(b,t,x)+\partial_b[v_3(b,T(t),x)\,y_3(b,t,x)] \\
-\beta\partial_b^2 y_3(b,t,x)-\mu_3\Delta y_3(b,t,x) \\
=-\theta_3(b,T(t),x)\,y_3(b,t,x), & (b,t,x)\in\alpha_3, \\
\partial_t y_4(b,t,x)+\partial_b[v_4(b,T(t),x)\,y_4(b,t,x)] \\
-\beta\partial_b^2 y_4(b,t,x)-\mu_4\Delta y_4(b,t,x) \\
=-\theta_4(b,T(t),x)\,y_4(b,t,x), & (b,t,x)\in\alpha_4,
\end{cases}
\tag{1.1}
$$

where

$$y_j(b,\,t,\,x),\quad 1\le j\le 4,$$

representing, respectively, the density of eggs, larvae, females and males of age b at time t in a geographical position x in the locust domain:

$$\theta_j(b,\,T(t),\,x),\quad 1\le j\le 4,$$

representing, respectively, the mortality rate of eggs, larvae, females and males of age b at temperature $T(t)$ in a geographical position x in the locust domain:

$$\gamma_j(b, T(t), x), \quad 1 \leq j \leq 2$$

representing the transition function of stage *j*; it is, in fact, the rate of individuals of age *b* at temperature $T(t)$ of stage *j* which pass to stage $j+1$ in a geographical position *x* of the domain and $\gamma_3(b, T(t), x)$, is the egg-laying rate:

$$v_j(b, T(t), x), \ 1 \leq j \leq 4,$$

representing the growth rate of individuals of age *b* at temperature $T(t)$ (at time *t*) of stage *j* in a geographical position *x* of the domain:

$$B_j, \ 1 \leq j \leq 4,$$

representing, respectively, the maximum age of individuals in stage j, β, μ_j and λ (sex ratio) which are positive constants and where $t \geq 0$. The diffusion coefficient μ_j represents the effects of dispersion of individuals or the different movements of individuals in space. Note also that Δ is the Laplace operator with respect to *x*.

The diffusion coefficient β represents the effects of dispersion or the various modifications in the organism of individuals during their development,

$$\alpha_j = (0, B_j) \times (0, +\infty) \times \Omega, \quad 1 \leq j \leq 4,$$

Ω is a non-empty bounded subset of $\mathbb{R}^n$ with $\Omega \subset \mathbb{R}^n$.

The boundary conditions and initial conditions are then expressed as follows:

$$
\begin{cases}
[v_1(b, T(t), x)y_1(b, t, x) - \beta\partial_b y_1(b, t, x)]_{b=0} \\
= \int_0^{B_3} \gamma_3(b, T(t), x)y_3(b, t, x)db, \\
[v_2(b, T(t), x)y_2(b, t, x) - \beta\partial_b y_2(b, t, x)]_{b=0} \\
= \int_0^{B_1} \gamma_1(b, T(t), x)y_1(b, t, x)db, \\
[v_3(b, T(t), x)y_3(b, t, x) - \beta\partial_b y_3(b, t, x)]_{b=0} \\
= \int_0^{B_2} \lambda\gamma_2(b, T(t), x)y_2(b, t, x)db, \\
[v_4(b, T(t), x)y_4(b, t, x) - \beta\partial_b y_4(b, t, x)]_{b=0} \\
= \int_0^{B_2} (1-\lambda)\gamma_2(b, T(t), x)y_2(b, t, x)db, \\
\partial_\eta y_j(b, t, x) = 0, \qquad (b, t, x) \in (0, B_j) \times (0, +\infty) \times \partial\Omega, \\
y_j(b, 0, x) = y_j^0(b, x), \quad (b, x) \in (0, B_j) \times \Omega, \ 1 \le j \le 4, \\
y_j(B_j, t, x) = 0, \qquad (t, x) \in (0, +\infty) \times \Omega, \ 1 \le j \le 4
\end{cases} \tag{1.2}
$$

with $t \ge 0$ and $\partial_\eta y_j(b, t, x) = \nabla y_j(b, t, x).\eta$, in which η represents the external normal. Here the following expression:

$$\int_0^{B_j} \lambda_j \gamma_j(b, T(t), x)y_j(b, t, x)db,$$

where $1 \le j \le 3$, designates respectively the distribution of larvae, females and eggs newborn at time *t* in a geographical position *x*, with

$$(\lambda_1, \lambda_2, \lambda_3) = (1, \lambda, 1).$$

We also have the following expression:

$$\int_0^{B_2} (1-\lambda)\gamma_2(b, T(t), x)y_2(b, t, x)db,$$

which designates the distribution of male newborns, where λ is the sex ratio.

Thus, for the mathematical analysis of our model, we make the following assumptions about the functions of the locust model:

H_1: Growth functions $v_j(b, T(t), x)$ are strictly positive and bounded,

$$0 < \min v_j < v_j(b, T(t), x) < \max v_j, \ \forall (b, t, x) \in \alpha_j, \ \ 1 \le j \le 4,$$

and there are positive constants A_j such that

$$\| \partial_b v_j(b, T(t), x) \|_\infty \le A_j, \ \ \forall (b, t, x) \in \alpha_j, \ \ 1 \le j \le 4.$$

H_2: The transition functions $\gamma_j(b, T(t), x), \ 1 \le j \le 4$ are also positive and bounded with respect to the age variable.

H_3: The functions of mortality $\theta_j(b, T(t), x), 1 \le j \le 4, \ \theta_j(b, T(t), x) \in L^\infty((0, B_j) \times (0, T) \times \Omega)$ and are positive as well.

H_4: The initial conditions $y_j^0(b, 0, x) \in L^2((0, B_j) \times \Omega)$ and are positive.

H_5: The temperature function $T(t)$ is measurable.

We recall that under these assumptions, we were able to prove the existence, uniqueness, positivity and regularity of the solution of (1.1) in [17].

2. Discretization of (1.1) and (1.2)

In this section, we first reduce the partial differential equation (PDE) to a finite-dimensional system of the form: $\dot{Y} = BY + GY$, where B and G are matrix and Y is the finite-dimensional state vector. So, to solve (1.1)-(1.2), we use the finite-difference method on $[0, B_j] \times \Omega$, for $1 \le j \le 4$. The discretization of (1.1), in space (dimension 1) and in age, is performed using the finite difference method on a rectangular grid $[0, B] \times [0, L]$, where $[0, L] \subset \Omega$. Thus, for a given rectangular grid Z with vertex (b_l, x_p), with

$1 \le l \le n$ and $1 \le p \le m$ and a uniform step size (without loss of generality) Δb, the discretization step with respect to the age variable in the direction of b and Δx the discretization step with respect to the space variable in the direction of x, we denote them by the grid diameter. We remind that the finite-difference method is the one that allows to pass from the continuous model to the discrete model by numerically performing the derivative operations involved in the continuous model. The finite-difference approximation of the aging term is given by

$$\frac{\partial^2 y_k(b_l, t, x_p)}{\partial b^2} = \frac{y_k(b_{l+1}, t, x_p) - 2y_k(b_l, t, x_p) + y_k(b_{l-1}, t, x_p)}{(\Delta b)^2},$$

with $1 \le k \le 4,\ 1 \le l \le n$ and $1 \le p \le m$.

Hence

$$\frac{\partial^2 y_k(b_l, t, x_p)}{\partial b^2} = \frac{y_k^{l+1, p} - 2y_k^{l, p} + y_k^{l-1, p}}{(\Delta b)^2},$$

with $1 \le k \le 4,\ 1 \le l \le n$ and $1 \le p \le m$.

Similarly, we have

$$\frac{\partial y_k(b_l, t, x_p)}{\partial b} = \frac{y_k(b_l, t, x_p) - y_k(b_{l-1}, t, x_p)}{\Delta b},$$

with $1 \le k \le 4,\ 1 \le l \le n$ and $1 \le p \le m$.

Also,

$$\frac{\partial y_k(b_l, t, x_p)}{\partial b} = \frac{y_k^{l, p} - y_k^{l-1, p}}{\Delta b},$$

with $1 \le k \le 4,\ 1 \le l \le n$ and $1 \le p \le m$.

The finite-difference approximation of the diffusion term is given by

$$\frac{\partial^2 y_k(b_l,\, t,\, x_p)}{\partial x^2} = \frac{y_k(b_l,\, t,\, x_{p+1}) - 2y_k(b_l,\, t,\, x_p) + y_k(b_l,\, t,\, x_{p-1})}{(\Delta x)^2},$$

with $1 \le k \le 4,\ 1 \le l \le n$ and $1 \le p \le m$.

Therefore

$$\frac{\partial^2 y_k(b_l,\, t,\, x_p)}{\partial x^2} = \frac{y_k^{l,\,p+1} - 2y_k^{l,\,p} + y_k^{l,\,p-1}}{(\Delta x)^2},$$

with $1 \le k \le 4,\ 1 \le l \le n$ and $1 \le p \le m$.

We also have

$$\frac{\partial y_k(b_l,\, t,\, x_p)}{\partial x} = \frac{y_k(b_l,\, t,\, x_p) - y_k(b_l,\, t,\, x_{p-1})}{\Delta x},$$

with $1 \le k \le 4,\ 1 \le l \le n$ and $1 \le p \le m$.

Thereafter

$$\frac{\partial y_k(b_l,\, t,\, x_p)}{\partial x} = \frac{y_k^{l,\,p} - y_k^{l,\,p-1}}{\Delta x},$$

with $1 \le k \le 4,\ 1 \le l \le n$ and $1 \le p \le m$.

Thus, with the discretization of age and space, we obtain

$$\partial_t y_1^{l,\,p} + y_1^{l,\,p}\partial_b \nu_1 + \nu_1^{l,\,p}\,\frac{y_1^{l,\,p} - y_1^{l-1,\,p}}{\Delta b} - \beta\,\frac{y_1^{l+1,\,p} - 2y_1^{l,\,p} + y_1^{l-1,\,p}}{(\Delta b)^2}$$

$$- \mu_1\,\frac{y_1^{l,\,p+1} - 2y_1^{l,\,p} + y_1^{l,\,p-1}}{(\Delta x)^2} = -[\theta_1^{l,\,p} + \gamma_1^{l,\,p}]\,y_1^{l,\,p}. \qquad (2.1)$$

First, we reason with the age in (2.1), which gives the following (2.2):

$$\partial_t y_1^{l,p} = -\left(\theta_1^{l,p} + \gamma_1^{l,p} + \partial_b v_1^{l,p} + \frac{v_1^{l,p}}{\Delta b} + \frac{2\beta}{(\Delta b)^2}\right) y_1^{l,p} + \left(\frac{v_1^{l,p}}{\Delta b} + \frac{\beta}{(\Delta b)^2}\right) y_1^{l-1,p} + \frac{\beta}{(\Delta b)^2} y_1^{l+1,p} \tag{2.2}$$

with

$$M_1 = \left(\theta_1^{l,p} + \gamma_1^{l,p} + \partial_b v_1^{l,p} + \frac{v_1^{l,p}}{\Delta b} + \frac{2\beta}{(\Delta b)^2}\right);$$

$$N_1 = \left(\frac{v_1}{\Delta b} + \frac{\beta}{(\Delta b)^2}\right) \text{ and } C_1 = \frac{\beta}{(\Delta b)^2}.$$

Hence, (2.2) becomes the following (2.3):

$$\partial_t y_1^{l,p} = N_1 y_1^{l-1,p} - M_1 y_1^{l,p} + C_1 y_1^{l+1,p}. \tag{2.3}$$

Reasoning with space, we obtain from (2.1) the equation below:

$$\partial_t y_1^{l,p} = \frac{\mu_1}{(\Delta x)^2}(y_1^{l,p+1} - 2y_1^{l,p} + y_1^{l,p-1}), \tag{2.4}$$

with $m_1 = \frac{\mu_1}{(\Delta x)^2}$, from which (2.4) becomes

$$\partial_t y_1^{l,p} = m_1(y_1^{l,p+1} - 2y_1^{l,p} + y_1^{l,p-1}). \tag{2.5}$$

(2.3) and (2.5) give the following matrix B_1:

$$B_1 = \frac{1}{2}\begin{pmatrix} -M_1-2m_1 & C_1+m_1 & \cdots & \cdots & \cdots & \cdots & 0 \\ N_1+m_1 & -M_1-2m_1 & C_1+m_1 & 0 & 0 & 0 & 0 \\ 0 & N_1+m_1 & -M_1-2m_1 & C_1+m_1 & 0 & 0 & 0 \\ 0 & 0 & N_1+m_1 & -M_1-2m_1 & C_1+m_1 & 0 & 0 \\ 0 & 0 & 0 & N_1+m_1 & -M_1-2m_1 & C_1+m_1 & 0 \\ \vdots & \ddots & \ddots & \ddots & \ddots & \ddots & \vdots \\ 0 & \cdots & \cdots & \cdots & \cdots & N_1+m_1 & -M_1-2m_1 \end{pmatrix}.$$

Now for the construction of the different birth matrix we note either $y_{l,\,p}(t)$ or $y_k^{l,\,p}(t)$ the approximation of $y_k(b_l,\,t,\,x_p)$ and

$$Y_j^{l,\,p}(t) = (y_k^{l,\,p}(t))_{1\le l\le n,\,1\le p\le m},$$

where $y_k^{l,\,p}$ is the position $l + p * (n-1)$ or $p + l * (m-1)$, $1 \le k \le 4$, B_k is the matrix of the mortality approximation, the diffusion approximation and the aging approximation. Therefore, the integral

$$\int_0^{B_3} \gamma_3 y_3 db$$

is approximated by

$$\int_0^{B_3} \gamma_3 y_3 db = \left(\frac{B_3}{n}\right)\sum_{l=1}^{n-1} \gamma_3(b_l,\,t,\,x_p)\,y_3(b_l,\,t,\,x_p) + \frac{\gamma_3(0)\,y_3(0,\,t,\,x_p) + \gamma_3(B_3)\,y_3(B_3,\,t,\,x_p)}{2}. \tag{2.6}$$

Thus, reasoning in the same way as (1.1), we obtain, respectively, for the second, the third and the fourth equation:

$$\int_0^{B_1} \gamma_1 y_1 db = \left(\frac{B_1}{n}\right)\sum_{l=1}^{n-1} \gamma_1(b_l,\,t,\,x_p)\,y_3(b_l,\,t,\,x_p) + \frac{\gamma_1(0)\,y_1(0,\,t,\,x_p) + \gamma_1(B_1)\,y_1(B_1,\,t,\,x_p)}{2}, \tag{2.7}$$

$$\int_0^{B_2} \lambda\gamma_2 y_2 db = \left(\frac{B_2}{n}\right)\sum_{l=1}^{n-1} \lambda\gamma_2(b_l,\,t,\,x_p)\,y_2(b_l,\,t,\,x_p) + \frac{\lambda\gamma_2(0)\,y_2(0,\,t,\,x_p) + \lambda\gamma_2(B_2)\,y_2(B_2,\,t,\,x_p)}{2}, \tag{2.8}$$

$$\int_0^{B_2} (1-\lambda)\gamma_2 y_2 db$$

$$= \frac{B_2}{n}\sum_{l=1}^{n-1}(1-\lambda)\gamma_2(b_l, t, x_p)y_2(b_l, t, x_p)$$

$$+ \frac{(1-\lambda)\gamma_2(0)y_2(0, t, x_p) + (1-\lambda)\gamma_2(B_2)y_2(B_2, t, x_p)}{2}. \tag{2.9}$$

We know previously that $Y = BY + GY$, where B and G are block matrix constructed from the matrix of each equation in (1.1). Note also that Y is the vector. With this in mind, let us construct our birth matrix for equation 1 of (1.1). From (1.2) and (2.6), we have

$$y_1^{0,p} = \frac{B_3}{v_1 n}\sum_{i=1}^{n-1}\gamma_3^{l,p}y_3^{l,p} + \frac{\gamma_3(0)y_3(0, t, x_p) + \gamma_3(B_3)y_3(B_3, t, x_p)}{2},$$

for $1 \le p \le m$.

And as

$$\frac{\partial y_1^{1,p}(t)}{\partial b} = \frac{y_1^{1,p}(t) - y_1^{0,p}(t)}{\Delta b},$$

then we have

$$\frac{\partial y_1^{1,p}(t)}{\partial b}$$

$$= \frac{y_1^{1,p}(t) - \frac{B_3}{v_1 n}\sum_{l=1}^{n-1}\gamma_3^{l,p}y_3^{l,p} + \frac{\gamma_3(0)y_3(0,t,x_p) + \gamma_3(B_3)y_3(B_3,t,x_p)}{2}}{\Delta b},$$

for $1 \le p \le m$.

Taking into account the births, we obtain the matrix G_1 of the equality resulting from equation (1) of (2.1) which will be given later. And by the

same reasoning as for equation (1) of (1.1) we obtain the matrix B_i, with $2 \leq i \leq 4$, which represents respectively the matrices of equations (2), (3) and (4).

Now, we provide the representation of the birth matrices G_1, G_2, G_3 and G_4.

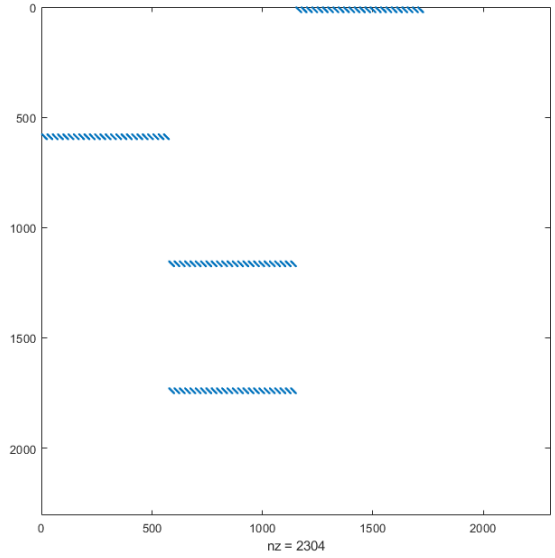

Figure 1. Matrix representing the renewal of the population of each stage.

Finally, the global matrix of (1.1) is given by

$$F = \begin{pmatrix} (B_1) & \begin{pmatrix} 0 \cdots 0 \\ \\ 0 \cdots 0 \end{pmatrix} & (G_1) & \begin{pmatrix} 0 \cdots 0 \\ \\ 0 \cdots 0 \end{pmatrix} \\ (G_2) & (B_2) & \begin{pmatrix} 0 \cdots 0 \\ \\ 0 \cdots 0 \end{pmatrix} & \begin{pmatrix} 0 \cdots 0 \\ \\ 0 \cdots 0 \end{pmatrix} \\ \begin{pmatrix} 0 \cdots 0 \\ \\ 0 \cdots 0 \end{pmatrix} & (G_3) & (B_3) & \begin{pmatrix} 0 \cdots 0 \\ \\ 0 \cdots 0 \end{pmatrix} \\ \begin{pmatrix} 0 \cdots 0 \\ \\ 0 \cdots 0 \end{pmatrix} & (G_4) & \begin{pmatrix} 0 \cdots 0 \\ \\ 0 \cdots 0 \end{pmatrix} & (B_4) \end{pmatrix}.$$

3. Convergence

To address the issue of convergence, we begin by returning to the discretization and approximation problem in order to determine the consistency error. To do this, let us assume that our solution y_j is of class C^4 for all $1 \leq j \leq 4$.

3.1. Consistency of the numerical scheme

The notion of consistency is directly linked to the truncation error of a numerical scheme, that is the error made when discretizing derivative terms. This error is generated when we choose the order of precision of the discretization, that is to say that the term from which we neglect the rest of the limited development we have found. The error made by truncating terms from a certain rank (2, 3, 4, 5, 6, 7 and so on) is called the *truncation error*. A scheme is said to be consistent if this error decreases with the approximation step (b, x or t). Consistency characterizes the way in which the finite difference equation (FDE) approaches the partial differential equation (PDE). A numerical scheme of the exact FDE equation tends towards the PDE when the age, time and space discretization steps independently tend towards zero. The study of consistency then becomes a step in the study of the convergence of the numerical solution of the finite-difference scheme to the exact solution of the equation. To do this, let us take a look at the order of consistency of our digital diagram. We can now state the following theorem.

Theorem 3.1. *Under the assumption that our solution* y_j *is of class* C^4 *with* $1 \leq j \leq 4$, *our numerical scheme is consistent of order two in space and age and consistent of order one in time.*

Proof of Theorem 3.1. We reason with the first equation of (1.1). Using the formula of Taylor, it follows, respectively, for time, age and space that

$$\frac{\partial y_1(b, t, x)}{\partial t} = \frac{y_1(b, t + \Delta t, x) - y_1(b, t, x)}{\Delta t} + \varepsilon(\Delta t), \tag{3.1}$$

with

$$\varepsilon(\Delta t) = -\frac{\Delta t}{2}\frac{\partial^2 y_1(b,\,\Theta,\,x)}{\partial t^2},$$

this scheme is then both explicit and of order 1,

$$\frac{\partial y_1(b,\,t,\,x)}{\partial b} = \frac{y_1(b+\Delta b,\,t,\,x) - y_1(b,\,t,\,x)}{\Delta b} + \varepsilon(\Delta b), \tag{3.2}$$

where

$$\varepsilon(\Delta b) = -\frac{\Delta b}{2}\frac{\partial^2 y_1(\omega,\,t,\,x)}{\partial b^2}.$$

Subsequently, this scheme is also both explicit and of order 1,

$$\frac{\partial y_1(b,\,t,\,x)}{\partial x} = \frac{y_1(b,\,t,\,x+\Delta x) - y_1(b,\,t,\,x)}{\Delta x} + \varepsilon(\Delta x), \tag{3.3}$$

and

$$\varepsilon(\Delta x) = -\frac{\Delta x}{2}\frac{\partial^2 y_1(b,\,t,\,\eta)}{\partial x},$$

in the following, this scheme is also both explicit and of order 1. In the same way as for the first derivative, we obtain using the formula of Taylor, for the second derivative respectively for time, space and age as follows:

$$\frac{\partial^2 y_1(b,\,t,\,x)}{\partial t^2} = \frac{y_1(b,\,t-\Delta t,\,x) - 2y_1(b,\,t,\,x) + y_1(b,\,t+\Delta t,\,x)}{\Delta t^2} - \frac{\Delta t^2}{12}\frac{\partial^4 y_1(b,\,\Theta,\,x)}{\partial t^4}, \tag{3.4}$$

$$\frac{\partial^2 y_1(b,\,t,\,x)}{\partial x^2} = \frac{y_1(b,\,t,\,x-\Delta x) - 2y_1(b,\,t,\,x) + y_1(b,\,t,\,x+\Delta x)}{\Delta x^2} - \frac{\Delta x^2}{12}\frac{\partial^4 y_1(b,\,t,\,\eta)}{\partial x^4}, \tag{3.5}$$

$$\frac{\partial^2 y_1(b,\, t,\, x)}{\partial b^2} = \frac{y_1(b-\Delta b,\, t,\, x) - 2y_1(b,\, t,\, x) + y_1(b+\Delta b,\, t,\, x)}{\Delta b^2}$$

$$- \frac{\Delta b^2}{12} \frac{\partial^4 y_1(\omega,\, t,\, x)}{\partial b^4}, \tag{3.6}$$

with

$$\Theta \in [t-\Delta t;\, t+\Delta t], \quad \eta \in [x-\Delta x;\, x+\Delta x], \quad \omega \in [b-\Delta b;\, b+\Delta b].$$

Let us replace (3.1), (3.2), (3.3), (3.4), (3.5) and (3.6) obtained above in the first equation of (1.1) in order to obtain the consistency error. Recall that the first equation is

$$\partial_t y_1(b,\, t,\, x) + \partial_b[\nu_1(b,\, T(t),\, x)\, y_1(b,\, t,\, x)] - \beta \partial_b^2 y_1(b,\, t,\, x) - \mu_1 \Delta y_1(b,\, t,\, x)$$

$$= -[\theta_1(b,\, T(t),\, x) + \gamma_1(b,\, T(t),\, x)]\, y_1(b,\, t,\, x).$$

Thus, through several calculations, we get

$$\frac{y_1(b,\, t+\Delta t,\, x) - y_1(b,\, t,\, x)}{\Delta t} + \nu_1 \frac{y_1(b+\Delta b,\, t,\, x) - y_1(b,\, t,\, x)}{\Delta b}$$

$$- \beta \left[\frac{y_1(b-\Delta b,\, t,\, x) - 2y_1(b,\, t,\, x) + y_1(b+\Delta b,\, t,\, x)}{\Delta b^2} \right]$$

$$- \mu_1 \left[\frac{y_1(b,\, t,\, x-\Delta x) - 2y_1(b,\, t,\, x) + y_1(b,\, t,\, x+\Delta t)}{\Delta x^2} \right]$$

$$+ [\theta_1(b,\, T(t),\, x) + \gamma_1(b,\, T(t),\, x)]\, y_1(b,\, t,\, x)$$

$$= \frac{1}{2} \left[\frac{\Delta t\, \partial^2 y_1(b,\, \Theta,\, x)}{\partial t^2} + \nu_1 \frac{\Delta b \partial^2 y_1(\omega,\, t,\, x)}{\partial b^2} \right]$$

$$- \frac{1}{12} \left[\beta \frac{\Delta b^2 \partial^4 y_1(\omega,\, t,\, x)}{\partial b^4} + \mu_1 \frac{\Delta x^2 \partial^4 y_1(b,\, t,\, \eta)}{\partial x^4} \right]. \tag{3.7}$$

Therefore, we have

$$P_E(b,\, t,\, x) = \frac{1}{2}\left[\frac{\Delta t\,\partial^2 y_1(b,\, \Theta,\, x)}{\partial t^2} + \nu_1 \frac{\Delta b \partial^2 y_1(\omega,\, t,\, x)}{\partial b^2}\right]$$

$$-\frac{1}{12}\left[\beta \frac{\Delta b^2 \partial^4 y_1(\omega,\, t,\, x)}{\partial b^4} + \mu_1 \frac{\Delta x^2 \partial^4 y_1(b,\, t,\, \eta)}{\partial x^4}\right], \qquad (3.8)$$

with $P_E(b,\, t,\, x)$ being the consistency error.

Now with (3.7) we have the consistency error linked to space, which we denote by $P_{Ex} = \delta \Delta x^2$ which allows us to say that the numerical scheme is consistent of order 2 in space, here $\delta = -\frac{1}{12}\frac{\mu_1 \partial^4 y_1(b,\, t,\, \eta)}{\partial x^4}$. The consistency error linked to age denoted by $P_{Eb} = \xi \Delta b + \tau \Delta b^2$, which allows us to say that the numerical scheme is consistent of order 2 in age with $\tau = -\frac{1}{12}\frac{\beta \partial^4 y_1(\omega,\, t,\, x)}{\partial b^4}$ and $\xi = \frac{1}{2}\frac{\nu_1 \Delta b \partial^2 y_1(\omega,\, t,\, x)}{\partial b^2}$. Also the time-related consistency error $P_{Et} = \kappa \Delta t$ allows us to say that the numerical scheme is consistent of order 1 in time with $\kappa = \frac{1}{2}\frac{\partial^2 y_1(b,\, \Theta,\, x)}{\partial t^2}$. After a number of computations that have enabled us to obtain the order of consistency of our numerical scheme, the final conclusion is that the numerical scheme is consistent of order 2 in space and age and consistent of order 1 in time. Finally, if we make Δt, Δb, Δb^2 and Δx^2 tend towards 0 in (3.8), then we deduce that the scheme is consistent for equation 1 of (1.1). In the same way as the reasoning for the first equation of (1.1), we show that equations 2, 3 and 4 of (1.1) have their numerical schemes consistent of the same order.

3.2. Stability of the numerical scheme

Generally speaking, the stability of a numerical scheme is closely linked to the numerical error. The study of stability therefore makes it possible to

determine the amplification of errors committed by the numerical scheme. A numerical scheme is stable if the errors made at one computation time step do not increase the errors as the computation continues. On the other hand, if the errors increase with each iteration, then the scheme is said to be unstable. It should also be noted that the stability of a numerical method is a key aspect to consider when ensuring that the solutions produced are reliable and accurate. There are various criteria and methods for analyzing and ensuring stability, depending on the type of problem to be solved. Now let us talk about the domain stability condition.

In the case of our numerical scheme, we choose as a stability condition, to impose that the vector of approximate solutions be preserved or decreased in norm over time. In clearer terms, this means that by choosing this condition, we ensure that the numerical errors introduced by the scheme will not cause the solution to explode, which is crucial to ensure that the scheme remains faithful to the real solution of the problem.

Now let us give the following theorem.

Theorem 3.2. *Let us assume the following restriction*:

$$\Delta t \leq \frac{1}{\max\limits_{1\leq j\leq 4}\left(\dfrac{v_j}{\Delta b}+\dfrac{\beta}{(\Delta b)^2}+\dfrac{\mu_j}{(\Delta x)^2}+\theta_j+\gamma_j\right)}, \tag{3.9}$$

where θ_j, γ_j *and* v_j *representing respectively the mortality rate*, *the transition function*, *and the growth rate of individuals*. *Here*

$$\begin{cases} v_j = \max\limits_{1\leq i\leq n} v_j^i;\ \ \theta_j = \max\limits_{1\leq i\leq n} \theta_j^i;\ \ \gamma_j = \max\limits_{1\leq i\leq n} \gamma_j^i;\ \ \mu_j = \max\limits_{1\leq i\leq n} \mu_j^i, \\ r = v_j^i \dfrac{\Delta t}{\Delta b};\ \ g = \beta \dfrac{\Delta t}{(\Delta b)^2};\ \ h = \mu_j \dfrac{\Delta t}{(\Delta x)^2};\ \ d = \Delta t(\theta_j^i + \gamma_j^i). \end{cases}$$

Let $Q_1 = r - 2g - 2h - d + 1;\quad Q_2 = -r + g + h$ *and* $Q_3 = g + h,$ *with* $Q_1 \leq 1,\ Q_2 \leq 1$ *and* $Q_3 \leq 1,$ *such that* $\sum\limits_{j=1}^{3} Q_j = 1; Q_j \in \mathbb{R}_+$. *Thus*, *under the*

CFL (*Courant-Friedrichs-Lewy*) *stability condition*, *our numerical scheme is stable*.

Proof of Theorem 3.2. The discretization of a complete equation in (1.1) generally gives us the following numerical scheme:

$$\frac{y_j^{i+1}-y_j^i}{\Delta t}+v_j^i\frac{y_{j+1}^i-y_j^i}{\Delta b}-\beta\frac{y_{j+1}^i-2y_j^i+y_{j-1}^i}{(\Delta b)^2}$$

$$-\mu_j\frac{y_{j+1}^i-2y_j^i+y_{j-1}^i}{(\Delta x)^2}+[\theta_j^i+\gamma_j^i]y_j^i=0, \tag{3.10}$$

with $1\le i\le n$ and $1\le j\le 4$.

From (3.10) we obtain

$$y_j^{i+1}=\left(v_j^i\frac{\Delta t}{\Delta b}-2\beta\frac{\Delta t}{(\Delta b)^2}-2\mu_j\frac{\Delta t}{(\Delta x)^2}-\Delta t(\theta_j^i+\gamma_j^i)+1\right)y_j^i$$

$$+\left(-v_j^i\frac{\Delta t}{\Delta b}+\beta\frac{\Delta t}{(\Delta b)^2}+\mu_j\frac{\Delta t}{(\Delta x)^2}\right)y_{j+1}^i$$

$$+\left(\beta\frac{\Delta t}{(\Delta b)^2}+\mu_j\frac{\Delta t}{(\Delta x)^2}\right)y_{j-1}^i. \tag{3.11}$$

We remark that, the stability of our numerical scheme depends on the values of the parameters $(v_j^i,\beta,\mu_j,\theta_j^i,\gamma_j^i)$ as well as the discretization steps $(\Delta t,\Delta b,\Delta x)$. This means that to ensure the stability of our numerical scheme, the time step Δt as well as $(v_j^i,\beta,\mu_j,\theta_j^i,\gamma_j^i)$ must be sufficiently small compared to the space and age steps. Therefore, starting from (3.11) we have

$$y_j^{i+1}=(r-2g-2h-d+1)y_j^i+(-r+g+h)y_{j+1}^i+(g+h)y_{j-1}^i. \tag{3.12}$$

Recall that y_j^{i+1} is written as a convex combination of the three values y_{j-1}^i, y_j^i and y_{j+1}^i. Using the assumptions

$$(r - 2g - 2h - d + 1) + (-r + g + h) + (g + h) = 1 \tag{3.13}$$

and

$$\begin{cases} 0 \le r - 2g - 2h + 1 \le 1 \\ 0 \le -r + g + h \le 1 \\ 0 \le g + h \le 1, \end{cases} \tag{3.14}$$

with the various calculations, we obtain

$$0 \le r \le 1, \ \ 0 \le g \le 1, \ \ 0 \le h \le 1 \ \text{ and } \ d \le 1.$$

Thus, taking into account the previous calculations, we get

$$r = v_j^i \frac{\Delta t}{\Delta b} \le 1;\ g = \beta \frac{\Delta t}{(\Delta b)^2} \le 1;\ h = \mu_j \frac{\Delta t}{(\Delta x)^2} \le 1 \text{ and } d = \Delta t(\theta_j^i + \gamma_j^i) \le 1.$$

Moreover, the assumption (3.9) leads to

$$\Delta t \le \frac{1}{\dfrac{v_j}{\Delta b} + \dfrac{\beta}{(\Delta b)^2} + \dfrac{\mu_j}{(\Delta x)^2} + \theta_j + \gamma_j}.$$

In conclusion, our CFL stability condition is verified, which guarantees the stability of our numerical scheme.

Proposition 3.1. *Let us assume that the conditions of Theorem* 3.1 *and Theorem* 3.2 *are satisfied. Then according to Lax's theorem, we have convergence of our numerical schemes.*

Proof of Proposition 3.1. According to Lax's theorem, convergence is achieved since our numerical scheme satisfies the conditions of consistency and stability, in accordance with the assumptions of Theorems 3.1 and 3.2, thereby ensuring convergence.

4. Numerical Illustrations

For the simulation, we first present the initial conditions for eggs, larvae, females and males:

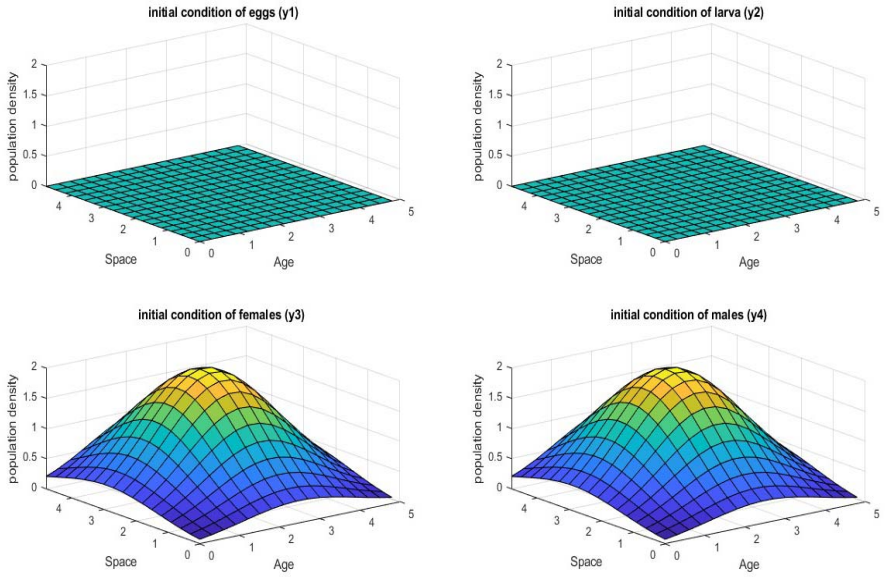

Figure 2. Initial conditions for eggs, larvae, females and males.

Figure 2 illustrates the variation of the densities of eggs, larvae, females, and males with respect to age and space, highlighting zones of optimal density. These visualizations provide valuable insights into population trends and behaviors, thereby supporting informed decision-making for species management. In particular, we observe that the densities of eggs (y_1) and larvae (y_2) are zero at the initial state indicating that neither eggs nor larvae are present.

We now present various diagrams showing the evolution of the number of eggs, larvae, and egg-laying events over time. These diagrams help illustrate the different numerical schemes. To do this, we consider γ_j, $1 \leq j \leq 3$.

For egg-laying

$$\gamma_3(b) = k\left(1 - \left(\frac{b - b_0}{w}\right)^2\right), \text{ with } k = 1,\ w = 3 \text{ and } b_0 = 3.$$

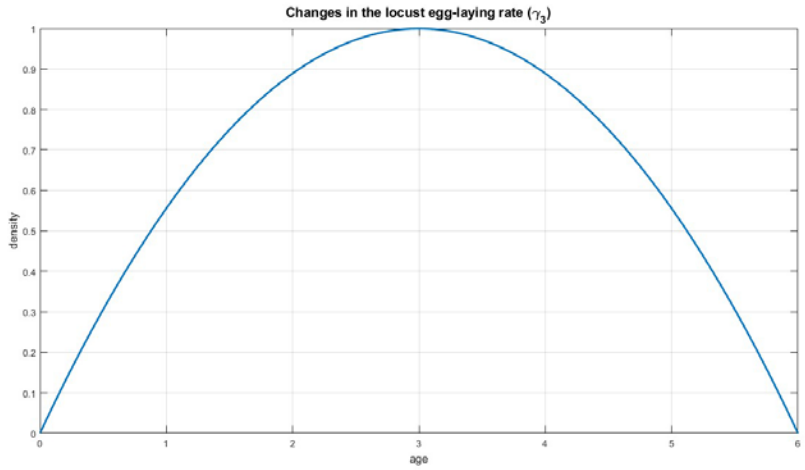

Figure 3. Curve representing the egg-laying rate $\gamma_3(b)$ of locusts as a function of age b.

The graph shows that the locusts' egg-laying rate is low at a young age, peaks at 3 month, and then decreases with age, reflecting their optimal reproduction period.

For the eggs

$$\gamma_1(b) = \begin{cases} 0, & \text{if } 0 \le b < 1, \\ k.e^{\left(\frac{-s(b-3)^2}{2n_1^2}\right)}, & \text{if } 1 \le b \le 2, \\ k.e^{\left(-\frac{(b-d)^2}{2n_1^2}\right)}, & \text{if } 2 < b \le 5, \\ 0, & \text{if } b > 5 \end{cases}$$

for representation, we take $k = 1$, $s = 1$, $d = 3.02$ and $n_1 = 1$.

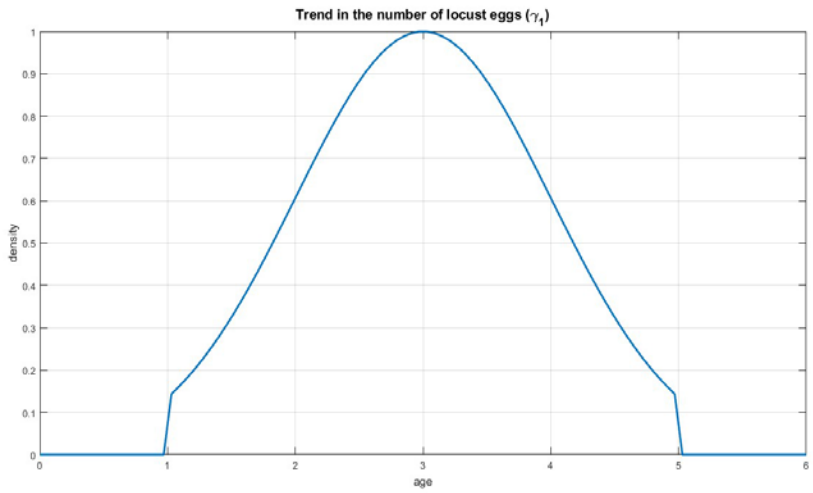

Figure 4. Curve representing the age distribution b of the eggs density $\gamma_1(b)$.

This figure illustrates the evolution of the stock of eggs already present in the soil. During the first 1 month, they remain in incubation with no significant hatching. Between 1 and 2 month, hatching begins and reaches a peak around month 2, before gradually slowing down. After 4 month, most of the eggs have hatched, and by 6 month, they have almost completely disappeared. The curve thus highlights a stable incubation phase, followed by progressive hatching, until the complete depletion of the egg stock.

For larvae

$$\gamma_2(b) = \begin{cases} 0, & \text{if } 0 \le b < 3, \\ k.e^{\left(\frac{-s(b-3)^2}{2n_2^2}\right)}, & \text{if } 3 \le b \le 4, \\ k.e^{\left(-\frac{(b-d)^2}{2n_2^2}\right)}, & \text{if } 4 < b \le 5, \\ 0, & \text{if } b > 5 \end{cases}$$

for representation of larvae: $k = 0.1$, $s = 1.2$, $d = 4.03$ and $n_2 = 0.5$.

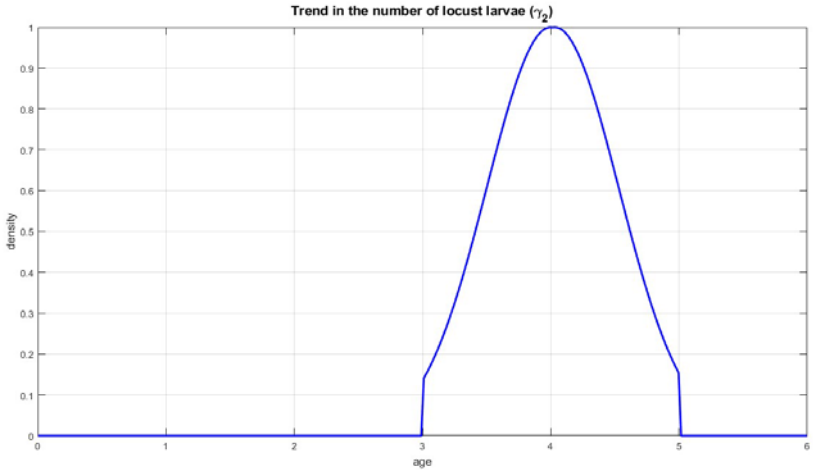

Figure 5. Curve representing the age distribution b of the larvae density $\gamma_2(b)$.

This figure illustrates the development of locust larvae. From 3 to 4 month, their population gradually increases, reaching a peak at 4 month, when most of the eggs have hatched. It then declines sharply due to natural mortality and the transition to the nymph stage. By 6 month, the larvae have almost disappeared, marking the completion of the transition to the next stage. The initial conditions are set as follows:

$$y_j^0(b, x) = 2e^{(-(0.15(b-3.5)^2+0.25(x-2.7)^2))}, \text{ with } 1 \le j \le 4,$$

which will be used in the calculations. The mortality functions θ_j, $1 \le j \le 4,$ are expressed as follows:

$$\theta_j(b, x) = \frac{1}{1+e^{-10(b-8)^2}} + (1 - 0{,}08x), \ 1 \le j \le 4$$

and the growth functions v_j, $1 \le j \le 4$ are expressed by $v_1 = 1.5$; $v_2 = 1.5$; $v_3 = 22$; $v_4 = 22$.

Example 4.1. So for the simulation of the states y_1, y_2, y_3 and y_4 of our system we consider

$$\begin{cases} \beta = 10^{-4}, \ \ n = 100, \\ \mu_1 = \mu_2 = \mu_3 = \mu_4 = 10^{-3}, \\ B_1 = 5, B_2 = 6, B_3 = B_4 = 7, \\ T = 20, nT = 2000, \Delta b = \dfrac{3}{10}, \Delta x = \dfrac{3}{10}, \\ CFL = 0.4. \end{cases}$$

We now present a series of figures showing the evolution of system at various time steps.

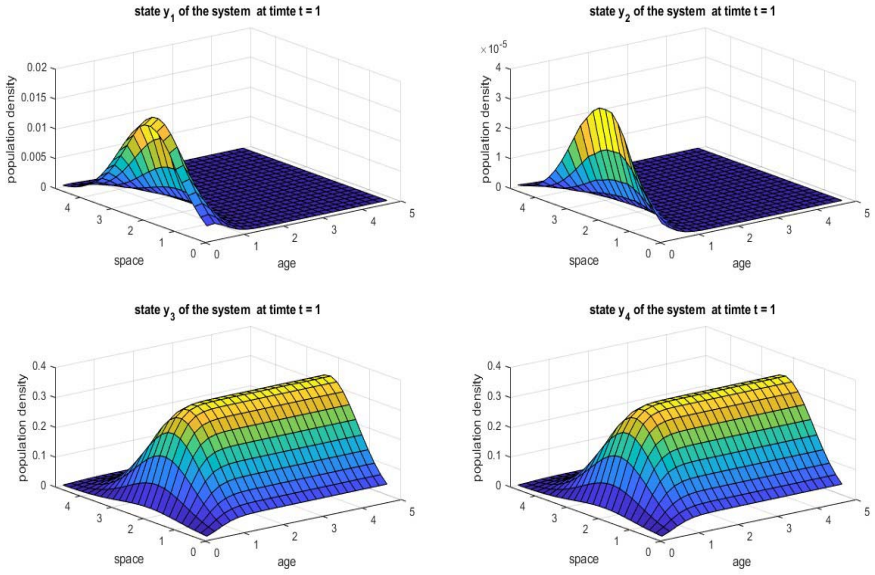

Figure 6. Evolution of the eggs (y_1), larvae (y_2), adult females (y_3) and adult males (y_4) for $t = 1$, highlighting the behavior in terms of the convergence of the numerical scheme.

These figures show that at time $t = 1$, a coherent dynamic of the desert locust life cycle is observed: a recent deposition of eggs (y_1) in a specific area indicates the beginning of oviposition by adult females (y_3), attracted

by favorable environmental conditions. The first hatchings give rise to larvae (y_2), still localized, reflecting an ongoing egg-to-larva transition. The females, either from a previous generation or having quickly reached adulthood, are present in the same areas as the eggs, confirming their reproductive role. Finally, the males (y_4), also concentrated in these regions, ensure a gender balance conducive to effective reproduction, illustrating the species typical gregarious behavior.

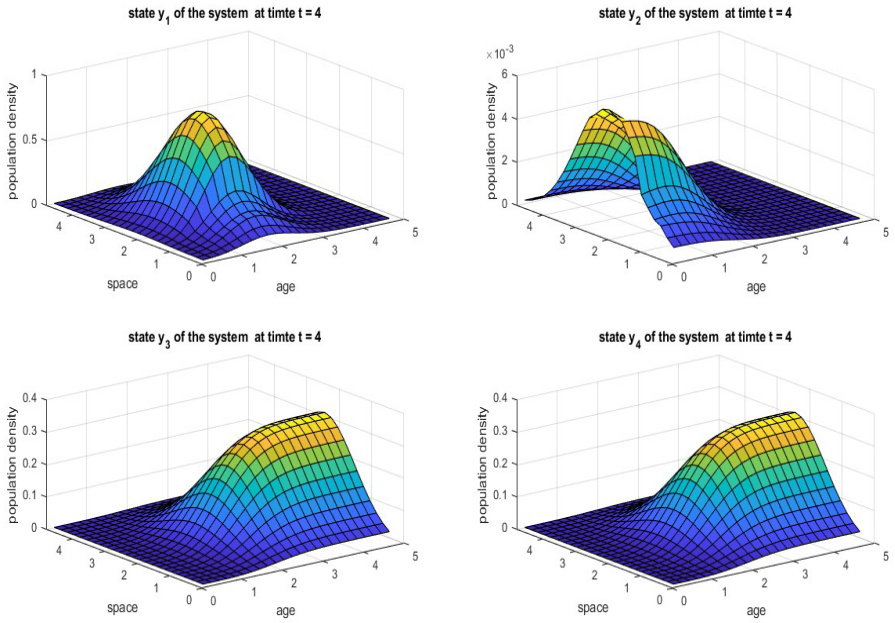

Figure 7. Evolution of the eggs (y_1), larvae (y_2), adult females (y_3) and adult males (y_4) for $t = 4$, highlighting the behavior in terms of the convergence of the numerical scheme.

These figures reveal a progressive transition toward hatching: the slight decrease in egg density (y_1) in certain areas indicates their progression to the larval stage. This phenomenon is accompanied by a spatio-temporal shift for the larvae (y_2), which emerge precisely in the regions where eggs were initially concentrated. At the same time, a gradual decrease in the density of

adult females (y_3) and males (y_4) can be observed, spreading in the direction of increasing age, which reflects the natural progression of the population dynamics.

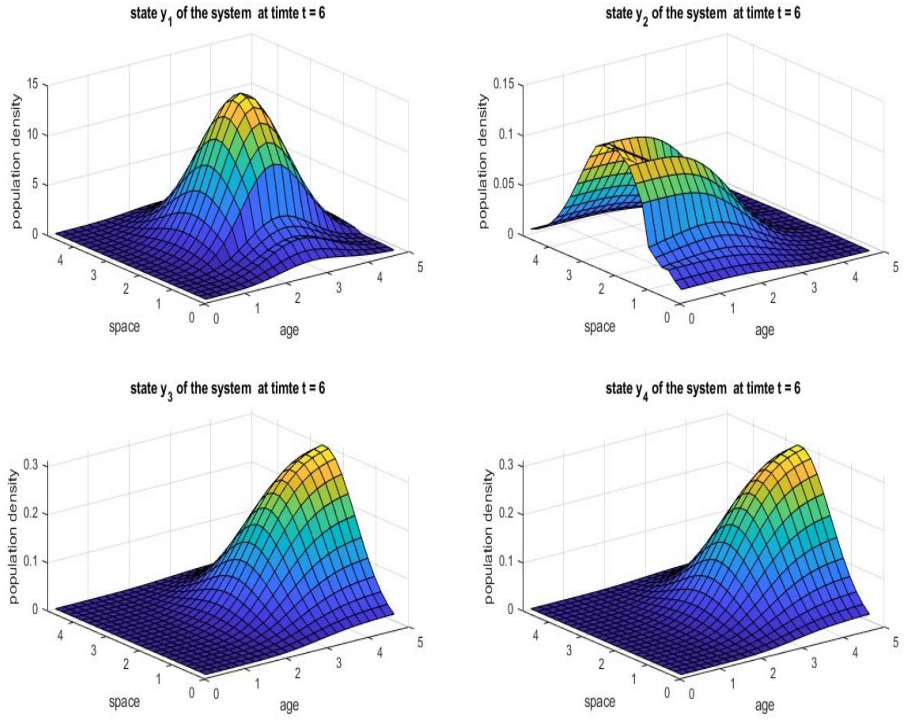

Figure 8. Evolution of the eggs (y_1), larvae (y_2), adult females (y_3), and adult males (y_4) for $t = 6$, highlighting the behavior in terms of the convergence of the numerical scheme.

At $t = 6$, the figures show a logical and gradual transition from eggs to larval stages and then to adulthood. A progressive decline in egg density is observed, due to either hatching or mortality. Simultaneously, the larvae reach a peak in density before decreasing as they mature into adults or die. Finally, the density of adult locusts (both females and males) gradually decreases as a result of aging and natural mortality.

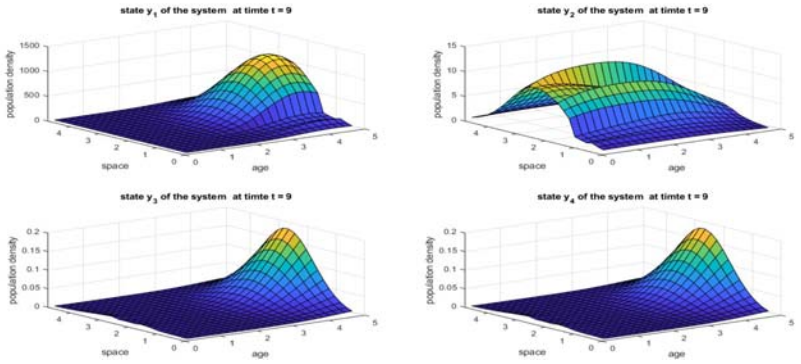

Figure 9. Evolution of the eggs (y_1), larvae (y_2), adult females (y_3) and adult males (y_4) for $t = 9$, highlighting the behavior in terms of the convergence of the numerical scheme.

Figure 9 shows that at time $t = 9$, a large portion of the eggs have already hatched, resulting in a relatively high larval density. These larvae continue to develop while moving through space. However, a gradual decrease in their density is observed, suggesting that mature larvae either transform into adult individuals (females or males) or die. As for the females and males, their population decreases with age, indicating a progressive disappearance due either to natural death or to migration out of the observed area.

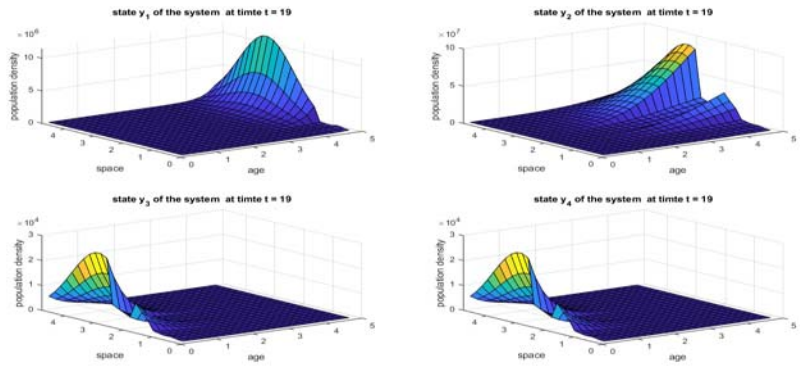

Figure 10. Evolution of the eggs (y_1), larvae (y_2), adult females (y_3) and adult males (y_4) for $t = 19$, highlighting the behavior in terms of the convergence of the numerical scheme.

Figure 10 shows that at time $t = 19,$ the density of eggs is extremely low or nearly zero, indicating the end of the incubation phase. A similar pattern is observed in the larvae, reflecting their transition to adult stages. Females and males, whose densities were nearly null just before this point, begin to reappear, signaling the resumption of their life cycle. This temporary disappearance may be due to natural mortality of the first adults or their movement outside the modeled area. Their reappearance marks the emergence of new adults from maturing larvae. This behavior is typical of age-structured populations, where different cohorts evolve at different rates, illustrating a generational succession in a dynamic environment.

The numerical schemes proposed above, evaluated at different given times, satisfy the convergence criteria by simultaneously ensuring consistency (through high-order discretizations) and stability (guaranteed by the CFL condition). The 3D simulations performed validate the proposed model by reproducing dynamics consistent with the initial biological assumptions and confirming the reliability of the theoretical and numerical approaches employed. Furthermore, let us recall that (3.9), which represents our CFL condition, implies that a CFL value greater than 1 leads to a loss of stability in our simulations. In some cases, this can even result in divergence or explosive instability in the figures, thereby compromising their accuracy and preventing convergence.

In what follows, we present a few illustrative examples of situations where the CFL condition is not satisfied, leading to divergence in our numerical schemes.

Example 4.2. In order to simulate the states y_1, y_2, y_3 and y_4 of our system, we take into account:

$$\begin{cases} \beta = 10^{-5}, \ \ n = 20, \\ \mu_1 = \mu_2 = \mu_3 = \mu_4 = 10^{-5}, \\ B_1 = 5, B_2 = 6, B_3 = B_4 = 7, \\ T = 10, nT = 200, \Delta b = \dfrac{7}{10}, \Delta x = \dfrac{7}{10}, \\ CFL = 2, \text{ or } CFL = 10, \\ v_1 = 100; v_2 = 100; v_3 = 500; v_4 = 500. \end{cases}$$

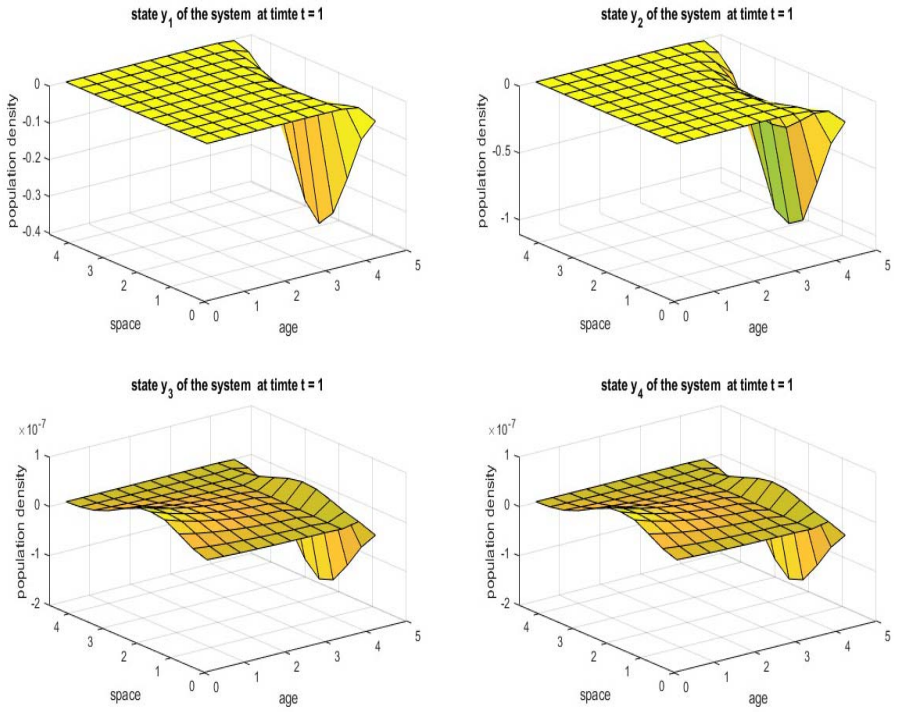

Figure 11. Evolution of the eggs (y_1), larvae (y_2), adult females (y_3) and adult males (y_4) for $t = 1$, highlighting the divergence behavior of the numerical scheme.

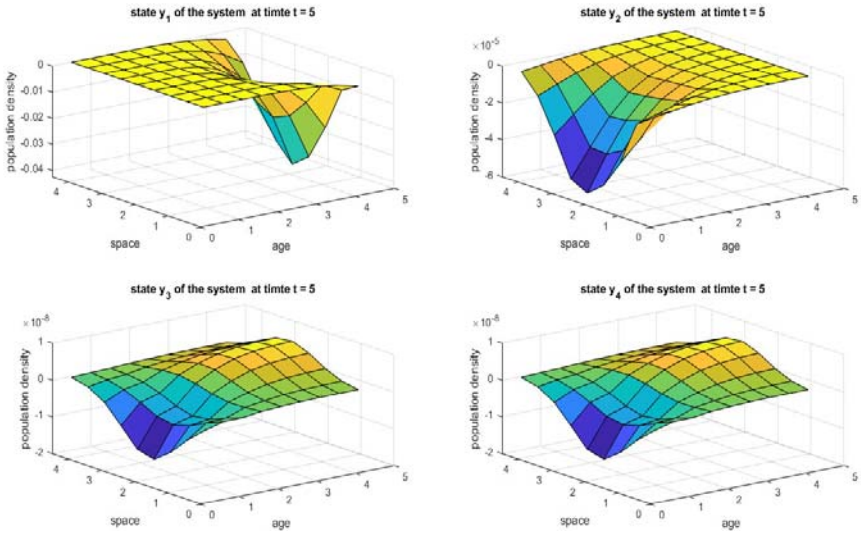

Figure 12. Evolution of the eggs (y_1), larvae (y_2), adult females (y_3) and adult males (y_4) for $t = 5$, highlighting the divergence behavior of the numerical scheme.

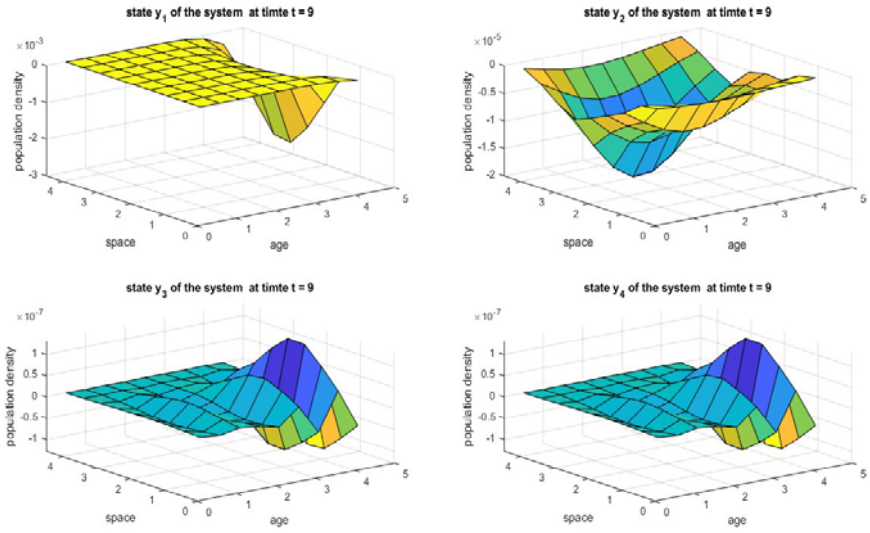

Figure 13. Evolution of the eggs (y_1), larvae (y_2), adult females (y_3) and adult males (y_4) for $t = 9$, highlighting the divergence behavior of the numerical scheme.

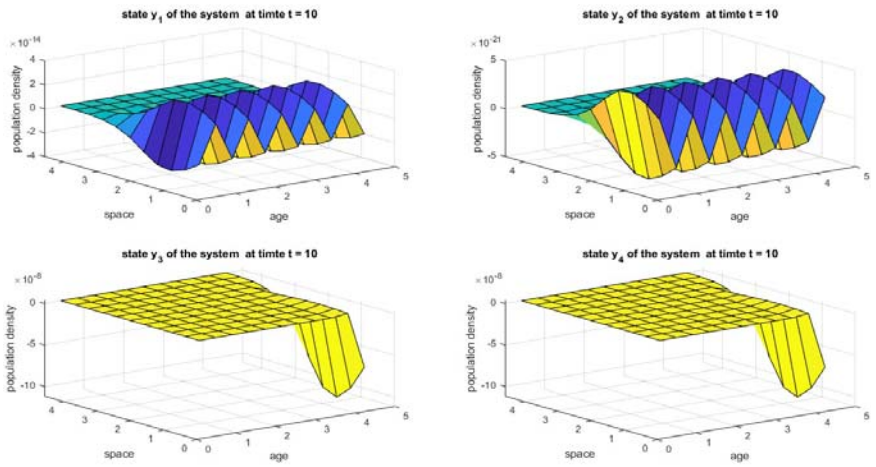

Figure 14. Evolution of the eggs (y_1), larvae (y_2), adult females (y_3) and adult males (y_4) for $t = 10$, highlighting the divergence behavior of the numerical scheme.

The figures clearly show that, if the Courant-Friedrichs-Lewy (CFL) condition is not satisfied in our case, numerical errors grow instead of dissipating. More precisely, if Δt is too large compared to Δb or Δx, then the terms g and h, or r, exceed their critical threshold. This leads to an exponential growth of errors, thereby compromising the stability of the scheme. Moreover, if the initial and boundary conditions are not properly implemented, then the scheme becomes unstable. Consequently, convergence cannot be guaranteed, thus rendering the numerical results unreliable.

Now let us make a global interpretation of the states:

Our codes model the population dynamics of locusts through different stages of their life cycle. Each sub-figure presents a key stage (egg, larva, adult female and adult male) with population density as a function of age and space. This allows us to observe how the population disperses or concentrates geographically, and how biological interactions (growth, diffusion, mortality) influence these populations. Our figures can be used to understand overall locust population behavior, which is important in the study of locust ecology and invasion control.

5. Conclusion

Starting from a population dynamics model of insect pests (locusts) structured in age, time and space, we were able to show the existence and uniqueness, the positivity of the solution in one of our papers [17] and now we continue the study by highlighting the numerical aspect using the finite difference method in this paper. We also note that in this manuscript convergence has been studied highlighting consistency and stability and various illustrations of schemes are given.

Acknowledgement

The authors would like to express their sincere gratitude to the anonymous referee for their careful reading of the manuscript and for their valuable suggestions and corrections to improve the quality of the paper.

References

[1] O. Angulo, J. C. López-Marcos, M. A. López Marcos and F. A. Milner, A numerical method for nonlinear age-structured population models with finite maximum age, Journal of Mathematical Analysis and Applications 361(1) (2010), 150-160.

[2] R. Courant, K. Friedrichs and H. Lewy, Über die partiellen differenzengleichungen der mathematischen physic, Mathematische Annalen 100(1) (1928), 32-74.

[3] R. Courant, K. Friedrichs and H. Lewy, On the partial difference equations of mathematical physics, IBM Journal of Research and Development 11(2) (1967), 215-234.

[4] R. Courant, E. Isaacson and M. Rees, On the solution of nonlinear hyperbolic differential equations by finite differences, Communications on Pure and Applied Mathematics 5(3) (1952), 243-255.

[5] K. Cressman, Desert locust, Biological and Environmental Hazards, Risks, and Disasters (2016), 87-105.

[6] E. Fernandez-Cara, R. Morales and D. A. Souza, Numerical null controllability of parabolic PDEs using Lagrangian methods. arXiv preprint arXiv:2411.14031, 2024.

[7] G. Gilioli, S. Pasquali and E. Marchesini, A modelling framework for pest population dynamics and management: An application to the grape berry moth, Ecological Modelling 320 (2016), 348-357.

[8] J. Guan, M. Li, X. Ju, J. Lin, J. Wu and J. Zheng. The potential habitat of desert locusts is contracting: predictions under climate change scenarios, Peer J. 9 (2021), e12311.

[9] M. Y. Kim and E. J. Park, An upwind scheme for a nonlinear model in age-structured population dynamics, Computers Mathematics with Applications 30(8) (1995), 5-17.

[10] E. Kimathi, H. E. Z. Tonnang, S. Subramanian, K. Cressman, E. M. Abdel-Rahman, M. Tesfayohannes, S. Niassy, B. Torto, T. Dubois, C. M. Tanga, M. Kassie, S. Ekesi, D. Mwangi and S. Kelemu, Prediction of breeding regions for the desert locust Schistocerca gregaria in east Africa, Scientific Reports 10(1) (2020), 11937.

[11] E. Lanzarone, S. Pasquali, G. Gilioli and E. Marchesini, A Bayesian estimation approach for the mortality in a stage-structured demographic model, Journal of Mathematical Biology 75(3) (2017), 759-779.

[12] P. D. Lax and R. D. Richtmyer, Survey of the stability of linear finite difference equations, In Selected Papers Volume I, Springer, 2005, pp. 125-151.

[13] S. Mechhoud, E. Witrant, L. Dugard and D. Moreau, Estimation de la diffusion thermique dans les plasmas de tokamak, In CIFA 2012-7ème Conférence Internationale Francophone d'Automatique, 2012.

[14] G. G. O'Brien, M. A. Hyman and S. Kaplan, A study of the numerical solution of partial differential equations, Journal of Mathematics and Physics 29(1-4) (1950), 223-251.

[15] S. Pasquali, C. Soresina and G. Gilioli, The effects of fecundity, mortality and distribution of the initial condition in phenological models, Ecological Modelling 402 (2019), 45-58.

[16] D. Picart and B. Ainseba, Parameter identification in multistage population dynamics model, Nonlinear Analysis: Real World Applications 12(6) (2011), 3315-3328.

[17] N. Ramdé, A. Traoré, Y. Simporé and O. Nakoulima, Existence and uniqueness of a solution for a four-stage age-structured population dynamics model with spatial diffusion for desert locusts, International Journal of Mathematics and Mathematical Sciences 2024(1) (2024), 8421625.

[18] K. Ren, L. Zhang and Y. Zhou, An energy-based discontinuous Galerkin method for the nonlinear Schrödinger equation with wave operator, SIAM Journal on Numerical Analysis 62(6) (2024), 2459-2483.

[19] A. T. Showler, Desert locust, Schistocerca gregaria forskål (orthoptera: Acrididae): plagues, Encyclopedia of Entomology (2008), pages 1181-1186.

[20] Y. Simporé, Null controllability of size-age dependent population dynamics models. arXiv preprint arXiv:2408.05291, 2024.

[21] Y. Simporé, Null controllability of a nonlinear population dynamics with age structuring and spatial diffusion, In Nonlinear Analysis, Geometry and Applications: Proceedings of the First NLAGA-BIRS Symposium, Dakar, Senegal, June 24-28, 2019, pages 1–33. Springer, 2020.

[22] Y. Simpore and A. Tambue, Null controllability and numerical method for crocco equation with incomplete data based on an exponential integrator and finite difference-finite element method, Computers and Mathematics with Applications 74(5) (2017), 1043-1058.

[23] P. M. Symmons and K. Cressman, Desert Locust Guidelines: Biology and Behaviour, FAO, Rome, 2001, pp. 1-42.

[24] A. Traoré, B. Ainseba and O. Traoré, Null controllability of a four stage and age-structured population dynamics model, Journal of Mathematics 2021(1) (2021), 5546150.

[25] A. Traore, B. Ainseba and O. Traore, On the existence of solution of a four-stage and age-structured population dynamics model, Journal of Mathematical Analysis and Applications 495(1) (2021), 124699.

[26] A. Traoré, O. S. Sougué, Y. Simporé and O. Traoré, Null Controllability of a Nonlinear Age Structured Model for a Two-sex Population, In Abstract and Applied Analysis, Vol. 2021, Wiley Online Library, 2021, p. 6666942.

[27] P. Y. Lagrée, Résolution numérique des équations de saint-venant, mise en oeuvre en volumes fnis par un solveur de riemann bien balance, Institut Jean Le Rond D'Alembert, 2020.